Journal of Computational Physics 229 (2010) 3675–3690

Contents lists available at ScienceDirect

Journal of Computational Physics

journal homepage: www.elsevier.com/locate/jcp

The Shortley–Weller embedded finite-difference method for the 3D Poisson equation with mixed boundary conditions

Z. Jomaa, C. Macaskill *

School of Mathematics and Statistics, University of Sydney, NSW 2006, Australia

ARTICLE INFO

Article history:
Received 28 October 2008
Received in revised form 12 January 2010
Accepted 19 January 2010
Available online 25 January 2010

Keywords:
Finite differences
Mixed boundary conditions
Poisson equation
Embedding
Irregular boundaries

ABSTRACT

This paper describes a method for the solution of the 3D Poisson equation, subject to mixed boundary conditions, on an irregularly shaped domain. A finite difference method is used, with the domain embedded in a rectangular grid. Quadratic treatment of the boundary conditions is shown to be necessary to obtain uniform error of $\mathcal{O}(\Delta^2)$. This contrasts with the Dirichlet case where both quadratic and linear treatments give $\mathcal{O}(\Delta^2)$ error, although the coefficient of error may be much larger for the linear case. Explicit error estimates demonstrating this behaviour are found for the 1D case with similar behaviour found in 2D and 3D numerical examples. Finally, the extension of this approach to the N-dimensional case is given, where $N > 3$.

1. Introduction

In this paper, we consider the 3D Poisson equation on an irregular domain with mixed boundary conditions, using an embedding method on a rectangular Cartesian grid (x, y, z) and employing a quadratic boundary treatment throughout. For all internal grid points, we use the standard seven-point stencil for the Laplace operator whereas the more general Shortley–Weller discretisation [25] is used for grid points adjacent to the boundary. This approach has been explored extensively for the special case of Dirichlet boundary conditions (see, e.g. [14]). However, for the case of mixed boundary conditions, the additional difficulty is that the boundary values of the solution are in general unknown, so that the method needs modification, as the Shortley–Weller discretisation is written in terms of these unknown values. Consider, for example, the Robin boundary condition $\beta\partial\psi/\partial n + \psi = \gamma$, where ψ is the unknown solution of the Poisson equation and β and γ are given constants. Here the boundary condition gives a relation between the normal derivative $\partial\psi/\partial n$ and the boundary value of ψ at every point on the boundary. At each grid point adjacent to the boundary, there are in general three such values of ψ required, one for each coordinate direction. (There may in fact be only one or two adjacent boundary points, but the method described here simplifies in an obvious way.) Our approach is to expand ψ around the grid point adjacent to the boundary using a quadratic polynomial in x, y and z involving nine unknown constants. Using this expansion first in the three boundary conditions, secondly at the six interior grid points adjacent to the chosen grid point and finally at the three adjacent boundary points gives a 12×12 matrix equation, with unknowns the three boundary values of ψ and the nine unknown coefficients in the quadratic expansion. Remarkably enough, this system decouples to the extent that the determination of the boundary values of ψ can be found from the inversion of a 3×3 system without the need to determine the constants involved in the quadratic expansion (although these can be found if required). This result generalises to N dimensions and furthermore the case $N = 2$ gives a 2×2 system that can be immediately inverted.

* Corresponding author.
E-mail address: c.macaskill@maths.usyd.edu.au (C. Macaskill).

0021-9991/$ - see front matter © 2010 Elsevier Inc. All rights reserved.
doi:10.1016/j.jcp.2010.01.021

The above approach determines the boundary values of ψ in terms of the normal derivative $\partial\psi/\partial n$ at the boundary. In turn the normal derivative at the boundary is expressed in terms of the ψ values at the internal nodes used by the Shortley–Weller discretisation. A method for approximating the normal derivative to $\mathcal{O}(\Delta)$ was given by Batschelet [2], where Δ is the grid spacing. Viswanathan [26] (see also Fox [11]) made use of the tangential derivative of the normal boundary condition to solve the Poisson equation to $\mathcal{O}(\Delta^2)$ but his formulation was evaluated at non-grid points, therefore needing further interpolation. In [5] this approach was refined for the Neumann problem, removing the need to use non-grid points, but retaining the use of the tangential derivative of the normal boundary condition. Furthermore, this formulation was of positive type (i.e. the coefficient matrix is a modified form of M-matrix (see e.g.[6])) which gives a more complicated formulation than that used here, but has the advantage of guaranteeing convergence for iterative methods. In [4], the authors extended these ideas to give an $\mathcal{O}(\Delta)$ and an $\mathcal{O}(\Delta^2)$ finite difference method for the Dirichlet and mixed boundary value problems for 2D elliptic second-order partial differential equations. A higher order finite difference method of a similar type was presented by Van Linde [18].

Greenspan [12] was able to avoid use of the tangential derivative of the normal boundary condition, by using a quadratic Taylor series approximation to obtain an $\mathcal{O}(\Delta^2)$ treatment of the normal derivative involving only internal grid point value and boundary values. He found that this was preferable to the linear treatment because of the higher accuracy obtainable. In the 2D case, our approach turns out to be equivalent to that of Greenspan [12], albeit for slightly different boundary conditions, because our treatment of the normal derivative is the same. In essence, our 3D results can be regarded as a generalisation of his 2D approach.

The work of [8] (2D) and [9] (3D) is a generalisation of that of [17], in that they deal with more general boundary conditions, but these approaches are only first-order accurate. A numerical method for the variable Poisson equation was developed in [19] to deal with more general boundary conditions in the presence of interfaces, but this method is again first-order accurate. Another approach solves the Poisson equation with mixed boundary condition by finding the particular solution to the non-homogeneous terms [1]. A second-order finite difference method for mixed boundary value problems is presented in [21,3]. It is not obvious how to extend these last two papers to 3D. Both papers avoid differentiation of the Neumann data, as does the present scheme, and have the advantage of using a positive type resulting matrix, with [3] giving a more compact system matrix. The 2D version of our scheme is much simpler but does not lead to an M-matrix. More recent papers deal with the mixed boundary conditions using a thin interface approach [22] or a fictitious domain method with a spread interface approach [23]. Both these last two methods are first-order accurate.

In this paper, we present a uniformly $\mathcal{O}(\Delta^2)$ 3D algorithm for the Poisson equation, using a quadratic boundary treatment and show how the 1D and 2D formulations can be obtained as special cases. For comparison purposes we also give the corresponding linear boundary treatment [7]. The numerical results confirm the expected $\mathcal{O}(\Delta^2)$ convergence for 2D and 3D problems with quadratic boundary treatment, while the 2D and 3D algorithms with linear boundary treatment give $\mathcal{O}(\Delta)$ convergence. This contrasts with the Dirichlet case, where the overall convergence rate is $\mathcal{O}(\Delta^2)$ for both quadratic and linear boundary treatments. This follows because although the Dirichlet boundary error is $O(\Delta^3)$ for the quadratic boundary formulation as against $\mathcal{O}(\Delta^2)$ for the linear boundary formulation [10,20], internal error is $\mathcal{O}(\Delta^2)$ in both cases. The loss of one order of convergence at the boundary in the Robin problem for both quadratic and linear boundary treatment can be understood from the 1D formulation (30) and (36). In Section 2.2, we give the explicit 1D error expression for both quadratic and linear boundary treatment following [14].

Finally, the general N-dimensional algorithm of $\mathcal{O}(\Delta^2)$ is given, from which the 1D, 2D and 3D algorithms can be derived as special cases.

2. Mathematical formulation

Here we describe the 3D $\mathcal{O}(\Delta^2)$ algorithm for the solution of the Poisson problem in an irregular domain subject to mixed boundary conditions. As mentioned in the introduction, in 2D the method described here is essentially equivalent to that of [12]. In 2D there are also existing algorithms [4,18] which differ from that used here in their use of the tangential derivative of the mixed boundary condition, or through concentrating on ensuring a positive type matrix [21,3]. In all cases, we use the nearest neighbour internal grid points only, which provides the simplest $\mathcal{O}(\Delta^2)$ formulation, but gives rise to a non-positive resulting matrix, which is less satisfactory for iterative techniques.

We consider in detail the 3D formulation of the Poisson equation: the 1D and 2D formulations can then be obtained as special cases. Furthermore, unlike the Dirichlet case the mixed boundary condition formulation is not additive, in the sense that there is no immediate extension from 1D to 2D and then to 3D, due to the coupling arising from the normal derivative so that the 3D problem must be addressed directly. Once the 3D problem is understood, it turns out that the N-dimensional problem can be treated as a relatively straightforward extension, and so this general result is provided in the Appendix A.

2.1. Three-dimensional case

Consider the three-dimensional mixed boundary value problem for the Poisson equation

$$\nabla^2\psi = f(x,y,z) \quad \text{on } \Omega \tag{1}$$

subject to Robin boundary conditions

$$\beta\frac{\partial\psi}{\partial n}+\psi=\gamma \quad \text{on } \partial\Omega \tag{2}$$

where Ω is the irregular region embedded in a rectangular domain and $\partial\Omega$ is the boundary of the irregular region. Here β and γ may vary with location on the boundary and $\beta \geqslant 0$. We take a rectangular grid $x_i = i\Delta x, y_j = j\Delta y$ and $z_k = k\Delta z$, and for simplicity of description let $\Delta x = \Delta y = \Delta z = \Delta$. The embedding idea is to take $\psi = 0$ for grid points outside Ω so that in general there is a jump in ψ between boundary values and the external grid points. The crucial aspect of the present formulation is the discretisation of the normal derivative at $\partial\Omega$ which corresponds to the discretisation of the Poisson equation on internal points adjacent to the boundary. For points adjacent to the boundary ((i,j,k) in Fig. 1), we can use either a quadratic or a linear treatment. The 3D quadratic (Shortley–Weller) discretisation at (i,j,k) is given by

$$-\frac{2}{\Delta^2}\sum_{m=1}^{3}\left[\frac{1}{(1-\alpha_m)(2-\alpha_m)}\psi_m-\left(\frac{1}{1-\alpha_m}\right)\psi_{i,j,k}+\left(\frac{1}{2-\alpha_m}\right)\psi_{i-\delta_{m1},j-\delta_{m2},k-\delta_{m3}}\right]=f_{i,j,k}, \tag{3}$$

while the 3D linear (Collatz) discretisation at (i,j,k) is given by

$$\frac{1}{\Delta^2}\sum_{m=1}^{3}\left[\frac{1}{(1-\alpha_m)}\psi_m-\left(\frac{2-\alpha_m}{1-\alpha_m}\right)\psi_{i,j,k}+\psi_{i-\delta_{m1},j-\delta_{m2},k-\delta_{m3}}\right]=f_{i,j,k}, \tag{4}$$

where δ_{mi} is the Kronecker delta (here and throughout). For all other internal points we use the standard rectangular seven-point stencil for the Laplace operator.

Consider an internal grid point (i,j,k), where there is an adjacent jump in ψ in each of the positive x, y and z directions, respectively (see Fig. 1), so that the distance from $(i+1,j,k)$ to the first jump is $\alpha_1\Delta$, the distance from $(i,j+1,k)$ to the second jump is $\alpha_2\Delta$, and the distance from $(i,j,k+1)$ to the third jump is $\alpha_3\Delta$. We discretise the Poisson equation at (i,j,k) subject to the mixed boundary condition at each of the three jump points:

$$\beta_1\left(\frac{\partial\psi}{\partial n}\right)_1+\psi_1=\gamma_1,\quad \beta_2\left(\frac{\partial\psi}{\partial n}\right)_2+\psi_2=\gamma_2,\quad \beta_3\left(\frac{\partial\psi}{\partial n}\right)_3+\psi_3=\gamma_3. \tag{5}$$

Here

$$\left(\frac{\partial\psi}{\partial n}\right)_r=\left(\frac{\partial\psi}{\partial x}\right)_r n_{r1}+\left(\frac{\partial\psi}{\partial y}\right)_r n_{r2}+\left(\frac{\partial\psi}{\partial z}\right)_r n_{r3}, \tag{6}$$

where $r = 1,2,3$, $n_r = [n_{r1}, n_{r2}, n_{r3}]$ is the normal vector at the rth jump boundary point.

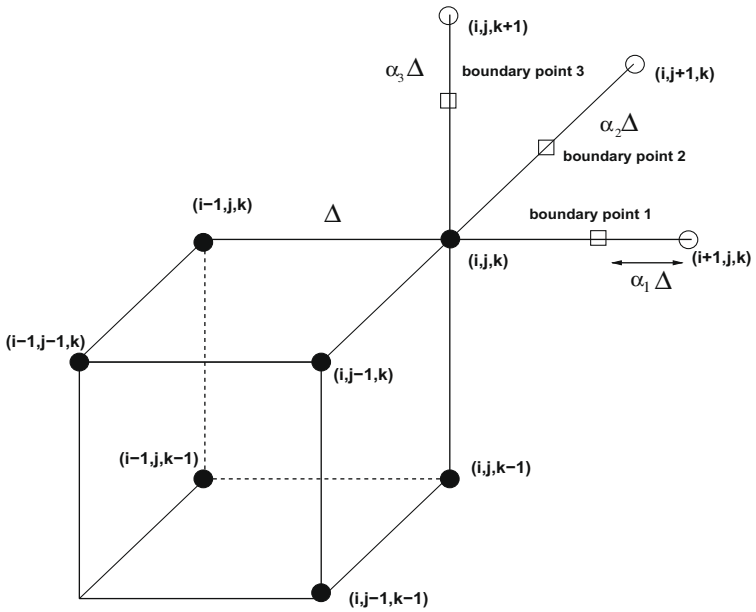

Fig. 1. Schematic of a typical 'corner point' of the 3D irregular domain. Filled circles represent interior grid points, open circles are exterior grid points, and the boxes are boundary points.

We need the boundary values ψ_1, ψ_2 and ψ_3 to complete the quadratic formulation of Eq. (3). To maintain $O(\Delta^2)$ accuracy, we must use a quadratic boundary treatment. Consider the quadratic approximation to the solution of the Poisson equation in the neighbourhood of the point (i,j,k):

$$\psi = \psi_{i,j,k} + c_1(x-x_i) + c_2(y-y_j) + c_3(z-z_k) + c_4(x-x_i)(y-y_j) + c_5(x-x_i)(z-z_k) + c_6(y-y_j)(z-z_k) + c_7(x-x_i)^2 + c_8(y-y_j)^2 + c_9(z-z_k)^2. \tag{7}$$

To obtain the boundary discretisation of the Poisson equation at (i,j,k) we solve the coupled problem of the determination of the constants $c_q, q = 1,\ldots,9$ and $\psi_r, r = 1,2,3$, i.e. 12 independent equations are required.

The first three equations are obtained by applying (7) in the boundary conditions (5) at the three boundary points adjacent to (i,j,k). For the first boundary condition we find

$$\psi_1 + \beta_1\left[\sum_{m=1}^{3} n_{1m}c_m + (1-\alpha_1)\Delta\left(\sum_{m=2}^{3} n_{1m}c_{m+2} + 2n_{11}c_7\right)\right] = \gamma_1 \tag{8}$$

with similar equations for the other two boundary conditions.

The next six equations are obtained by imposing (7) at the internal grid points adjacent to (i,j,k) in the order $(i-1,j,k),(i,j-1,k),(i,j,k-1),(i-1,j-1,k),(i-1,j,k-1),(i,j-1,k-1)$. We find for node $(i-1,j,k)$

$$c_1\Delta - c_7\Delta^2 = \psi_{i,j,k} - \psi_{i-1,j,k}, \tag{9}$$

with similar equations for nodes $(i,j-1,k)$ and $(i,j,k-1)$. For node $(i-1,j-1,k)$ we obtain

$$\Delta(c_1+c_2) - \Delta^2(c_4+c_7+c_8) = \psi_{i,j,k} - \psi_{i-1,j-1,k}, \tag{10}$$

again with similar equations for nodes $(i-1,j,k-1)$ and $(i,j-1,k-1)$. Finally, at the three boundary points ψ_r we have

$$\psi_r - (1-\alpha_r)\Delta c_r - (1-\alpha_r)^2\Delta^2 c_{r+6} = \psi_{i,j,k}, \quad r = 1,2,3. \tag{11}$$

Taking in order the quadratic approximations for the three boundary conditions of the form (8), the six interior conditions (9) and (10) and the three boundary values (11) gives a 12×12 system of equations:

$$\begin{pmatrix} I & BG & \Delta B(I-A)F_{3,M} & 2\Delta B(I-A)D \\ 0 & \Delta I & 0 & -\Delta^2 I \\ 0 & \Delta K_{M,3} & -\Delta^2 I_M & -\Delta^2 K_{M,3} \\ I & -\Delta(I-A) & 0 & -\Delta^2(I-A)^2 \end{pmatrix} \begin{pmatrix} \psi_1 \\ \psi_2 \\ \psi_3 \\ c_1 \\ c_2 \\ c_3 \\ c_4 \\ c_5 \\ c_6 \\ c_7 \\ c_8 \\ c_9 \end{pmatrix} = \begin{pmatrix} \gamma \\ p_1 \\ p_2 \\ p_3 \end{pmatrix}, \tag{12}$$

where I is the 3×3 identity matrix, 0 is the 3×3 zero matrix, and I_M is the 3×3 identity matrix in this case, because in general $M = N(N-1)/2$, where N is the dimensionality of the problem. We give the extension to N dimensions in the Appendix A. In (12) we have

$$A = \begin{pmatrix} \alpha_1 & 0 & 0 \\ 0 & \alpha_2 & 0 \\ 0 & 0 & \alpha_3 \end{pmatrix}, \quad B = \begin{pmatrix} \beta_1 & 0 & 0 \\ 0 & \beta_2 & 0 \\ 0 & 0 & \beta_3 \end{pmatrix}, \quad D = \begin{pmatrix} n_{11} & 0 & 0 \\ 0 & n_{22} & 0 \\ 0 & 0 & n_{33} \end{pmatrix},$$
$$F_{3,M} = \begin{pmatrix} n_{12} & n_{13} & 0 \\ n_{21} & 0 & n_{23} \\ 0 & n_{31} & n_{32} \end{pmatrix}, \quad G = \begin{pmatrix} n_{11} & n_{12} & n_{13} \\ n_{21} & n_{22} & n_{23} \\ n_{31} & n_{32} & n_{33} \end{pmatrix}, \quad K_{M,3} = \begin{pmatrix} 1 & 1 & 0 \\ 1 & 0 & 1 \\ 0 & 1 & 1 \end{pmatrix}, \tag{13}$$

and

$$\gamma = \begin{pmatrix} \gamma_1 \\ \gamma_2 \\ \gamma_3 \end{pmatrix}, \quad p_1 = \begin{pmatrix} \psi_{i,j,k} - \psi_{i-1,j,k} \\ \psi_{i,j,k} - \psi_{i,j-1,k} \\ \psi_{i,j,k} - \psi_{i,j,k-1} \end{pmatrix}, \quad p_2 = \begin{pmatrix} \psi_{i,j,k} - \psi_{i-1,j-1,k} \\ \psi_{i,j,k} - \psi_{i-1,j,k-1} \\ \psi_{i,j,k} - \psi_{i,j-1,k-1} \end{pmatrix}, \quad p_3 = \psi_{i,j,k}\begin{pmatrix} 1 \\ 1 \\ 1 \end{pmatrix}. \tag{14}$$

If we view the matrix in (12) as a four by four block matrix we can identify the sequence of row operations that is used to reduce (12) to (15). In summary we use row 2 of (12) to simplify row 3, then row 4 to simplify row 2. Row 4 is unchanged. We then use row 3 of (15) to eliminate column 3 of row 1, row 4 of (15) to eliminate column 4 of row 1 and finally row 2 of (15) to eliminate column 2 of row 1.

$$\begin{pmatrix} I+E & 0 & 0 & 0 \\ I & -\Delta(I-A)(2I-A) & 0 & 0 \\ 0 & 0 & \Delta^2 I_M & 0 \\ I & -\Delta(I-A) & 0 & -\Delta^2(I-A)^2 \end{pmatrix} \begin{pmatrix} \psi_1 \\ \psi_2 \\ \psi_3 \\ c_1 \\ c_2 \\ c_3 \\ c_4 \\ c_5 \\ c_6 \\ c_7 \\ c_8 \\ c_9 \end{pmatrix} = \begin{pmatrix} p_6 \\ p_5 \\ p_4 \\ p_3 \end{pmatrix}, \tag{15}$$

where E is a 3×3 matrix with entries

$$E_{rq} = \frac{\beta_r(1+2\delta_{rq}(1-\alpha_q))n_{rq}}{\Delta(1-\alpha_q)(2-\alpha_q)}, \quad r,q = 1,2,3 \tag{16}$$

with

$$\begin{aligned} p_4 &= \begin{pmatrix} \psi_{i-1,j-1,k} + \psi_{i,j,k} - \psi_{i-1,j,k} - \psi_{i,j-1,k} \\ \psi_{i-1,j,k-1} + \psi_{i,j,k} - \psi_{i-1,j,k} - \psi_{i,j,k-1} \\ \psi_{i,j-1,k-1} + \psi_{i,j,k} - \psi_{i,j-1,k} - \psi_{i,j,k-1} \end{pmatrix}, \\ p_5 &= (I-A)^2 \begin{pmatrix} \psi_{i-1,j,k} \\ \psi_{i,j-1,k} \\ \psi_{i,j,k-1} \end{pmatrix} + A(2I-A)p_3, \\ p_6 &= \gamma + \frac{1}{\Delta} B(I-A)(2Dp_1 - F_{3,M}p_4) + Ep_5. \end{aligned} \tag{17}$$

Now to obtain $\psi_r, r = 1,2,3$ we need to invert the 3×3 system of equations

$$(I+E)\begin{pmatrix} \psi_1 \\ \psi_2 \\ \psi_3 \end{pmatrix} = p_6 \tag{18}$$

which is done using computer algebra once and for all for any given boundary.

Substituting $\psi_r, r = 1,2,3$ in (3) completes the discretisation of the Poisson equation with Robin boundary conditions at any grid point (i,j,k) adjacent to three boundary points, with minor modifications required if, for example, (i,j,k) is adjacent to only one or two boundary points. For example, consider the case where (i,j,k) is adjacent to boundary point 1 and boundary point 2 but not boundary point 3. The equation describing the Robin boundary condition at boundary point 3 is no longer used, and secondly the equation at the boundary point 3 (from (11) with $r = 3$) is replaced by that for the corresponding internal point. We no longer have to find the value ψ at the corresponding boundary point, so reducing the number of unknowns by one also, giving rise to a system of 11 equations in 11 unknowns. Similarly for one boundary point only we find a 10×10 system.

From (18), or from the general form for N dimensions given in the Appendix A, the 1D and 2D formulations can be written down directly. For instance, in the 1D case, the matrices and vectors reduce to scalars. Because $M = 0, F_{1,M}, I_M$ and $K_{M,1}$ are null and

$$\begin{aligned} &A = \alpha_1, \quad B = \beta_1, \quad D = n_{11}, \\ &\gamma = \gamma_1, \quad p_1 = \psi_i - \psi_{i-1}, \quad p_3 = \psi_i \end{aligned} \tag{19}$$

with

$$E = \frac{\beta_1(3-2\alpha_1)n_{11}}{\Delta(1-\alpha_1)(2-\alpha_1)}. \tag{20}$$

In the 2D case, we have $M = 1$ so that $I_M = 1$ and the matrices become

$$A = \begin{pmatrix} \alpha_1 & 0 \\ 0 & \alpha_2 \end{pmatrix}, \quad B = \begin{pmatrix} \beta_1 & 0 \\ 0 & \beta_2 \end{pmatrix}, \quad D = \begin{pmatrix} n_{11} & 0 \\ 0 & n_{22} \end{pmatrix},$$
$$F_{2,1} = \begin{pmatrix} n_{12} \\ n_{21} \end{pmatrix}, \quad G = \begin{pmatrix} n_{11} & n_{12} \\ n_{21} & n_{22} \end{pmatrix}, \quad K_{1,2} = (1 \quad 1),$$
$$\gamma = \begin{pmatrix} \gamma_1 \\ \gamma_2 \end{pmatrix}, \quad p_1 = \begin{pmatrix} \psi_{i,j} - \psi_{i-1,j} \\ \psi_{i,j} - \psi_{i,j-1} \end{pmatrix}, \quad p_2 = (\psi_{i,j} - \psi_{i-1,j-1}), \quad p_3 = \psi_{i,j} \begin{pmatrix} 1 \\ 1 \end{pmatrix} \tag{21}$$

and

$$p_4 = (\psi_{i,j} + \psi_{i-1,j-1} - \psi_{i-1,j} - \psi_{i,j-1}). \tag{22}$$

The matrix E has elements given by

$$E_{rq} = \frac{\beta_r(1 + 2\delta_{rq}(1 - \alpha_q))n_{rq}}{\Delta(1 - \alpha_q)(2 - \alpha_q)}, \quad r, q = 1, 2. \tag{23}$$

Now to obtain $\psi_r, r = 1, 2$ we need to invert the 2×2 system of equations

$$(I + E)\begin{pmatrix} \psi_1 \\ \psi_2 \end{pmatrix} = p_6, \tag{24}$$

where

$$\begin{aligned} p_5 &= (I - A)^2 \begin{pmatrix} \psi_{i-1,j} \\ \psi_{i,j-1} \end{pmatrix} + A(2I - A)p_3, \\ p_6 &= \gamma + \frac{1}{\Delta} B(I - A)(2Dp_1 - F_{2,1}p_4) + Ep_5. \end{aligned} \tag{25}$$

In [15], a geometric approach is used that gives the same result as Eq. (24). Eq. (24) also agrees with the result that is found when the normal derivative $\partial\psi/\partial n$ is determined as in Greenspan [12]. This is expected, as he also used a 2D Taylor expansion.

For comparison purposes we also give the 3D linear formulation, using the 3D Collatz discretisation as in Eq. (4) with a linear treatment near the boundary:

$$\psi = \psi_{i,j,k} + c_1(x - x_i) + c_2(y - y_j) + c_3(z - z_j). \tag{26}$$

Use of a quadratic treatment like (7) near the boundary is possible but inconsistent, giving rise to a more complicated formulation, but still with $O(\Delta)$ error; this is therefore not pursued further here. Applying (26) to $(i, j - 1, k), (i, j, k - 1)$, boundary point 1 and the boundary condition at boundary point one gives

$$\left[1 + \frac{\beta_1 n_{11}}{(1 - \alpha_1)\Delta}\right]\psi_1 = \gamma_1 - \frac{\beta_1}{\Delta}\left[-\frac{n_{11}}{1 - \alpha_1} + n_{12} + n_{13}\right]\psi_{i,j,k} + \frac{\beta_1}{\Delta} n_{12}\psi_{i,j-1,k} + \frac{\beta_1}{\Delta} n_{13}\psi_{i,j,k-1}. \tag{27}$$

ψ_2 and ψ_3 are obtained in similar way. The 1D and 2D linear formulation can be determined directly from Eq. (27).

2.2. 1D error analysis

Consider the 1D Poisson equation $d^2\psi/dx^2 = f(x)$ for $x \in [x_L, x_R]$ embedded in the interval $[a, b]$, where the uniform grid spacing $\Delta \equiv \Delta x = (b - a)/\eta$ and there are $\eta + 1$ grid points such that $a = x_0 < x_L < x_1 < x_2 < \cdots < x_{\eta-2} < x_{\eta-1} < x_R < x_\eta = b$, with $x_L - x_0 = \alpha_L\Delta$ and $x_\eta - x_R = \alpha_R\Delta$. The solution ψ is set to zero outside $[x_L, x_R]$ and in general there are jumps at x_L and x_R where Robin boundary conditions are imposed. Here we discuss the 1D error expressions for ψ satisfying these boundary conditions, using the same approach as for the Dirichlet case first proposed in [16] and explicitly carried through in [14].

The 1D error $\xi = \psi - \psi^e$, where ψ^e and ψ are the exact and approximate solutions, respectively, satisfies

$$L\xi = \tau, \tag{28}$$

with L the discrete second derivative operator and τ the truncation error, subject to the immersed boundary conditions

$$-\beta_L \frac{d\xi}{dx}\bigg|_{x=x_L} + \xi_L = 0, \quad \beta_R \frac{d\xi}{dx}\bigg|_{x=x_R} + \xi_R = 0. \tag{29}$$

Here β_L and β_R play the same role as β_1 in (19).

We now summarise explicit results for the 1D error $\xi = \psi - \psi^e$, defined in Eq. (28) and subject to the boundary conditions (29). These are found using similar techniques to those employed for the Dirichlet case in [14] Section 2.2.1 and are discussed more extensively in [15].

When a quadratic treatment of the boundary conditions is used, we find

$$\xi_i = \Delta^2\left[\left(i-\alpha_L+\frac{\beta_L}{\Delta}\right)\frac{H_{\eta-1/2}}{\Delta}-\sum_{j=2}^{\eta-1}\left(j-\alpha_L+\frac{\beta_L}{\Delta}\right)\tau_j-\sum_{j=i+1}^{\eta-1}(i-j)\tau_j-\frac{(1-\alpha_L)(2-\alpha_L)\Delta+\beta_L(3-2\alpha_L)}{2\Delta}\tau_1\right]$$
$$\text{for } 1\leqslant i\leqslant \eta-1 \tag{30}$$

with

$$H_{\eta-1/2} = \Delta^2\left\{\sum_{j=2}^{\eta-1}\left(j-\alpha_L+\frac{\beta_L}{\Delta}\right)\tau_j+\frac{\alpha_R(1-\alpha_R)\Delta-\beta_R(1-2\alpha_R)}{2\Delta}\tau_{\eta-1}+\frac{(1-\alpha_L)(2-\alpha_L)\Delta+\beta_L(3-2\alpha_L)}{2\Delta}\tau_1\right\}$$
$$\times\left[(\eta-\alpha_L-\alpha_R)\Delta+\beta_L+\beta_R\right]^{-1}. \tag{31}$$

Rewriting as a sum of terms like those in the Dirichlet case and terms proportional to β we find:

$$\xi_i = \Delta^2\left[(i-\alpha_L)\frac{H_{\eta-1/2}}{\Delta}-\sum_{j=i+1}^{\eta-1}(i-j)\tau_j-\sum_{j=2}^{\eta-1}(j-\alpha_L)\tau_j-\frac{(1-\alpha_L)(2-\alpha_L)}{2}\tau_1\right]+\beta_L\Delta\left[\frac{H_{\eta-1/2}}{\Delta}-\sum_{j=2}^{\eta-1}\tau_j-\frac{(3-2\alpha_L)}{2}\tau_1\right], \tag{32}$$

where

$$H_{\eta-1/2} = \Delta^2\left\{\sum_{j=2}^{\eta-1}(j-\alpha_L)\tau_j+\frac{\alpha_R(1-\alpha_R)}{2}\tau_{\eta-1}+\frac{(1-\alpha_L)(2-\alpha_L)}{2}\tau_1\right\}\times\left[(\eta-\alpha_L-\alpha_R)\Delta+\beta_L+\beta_R\right]^{-1}$$
$$+\Delta\left[\sum_{j=2}^{\eta-1}\beta_L\tau_j+\frac{\beta_L(3-2\alpha_L)}{2}\tau_1-\frac{\beta_R(1-2\alpha_R)}{2}\tau_{\eta-1}\right]\times\left[(\eta-\alpha_L-\alpha_R)\Delta+\beta_L+\beta_R\right]^{-1}, \tag{33}$$

and

$$\tau_1 = -\frac{\Delta}{3}\alpha_L(\psi_1^e)''' - \frac{\beta_L(1-\alpha_L)(2-\alpha_L)\Delta}{3[(1-\alpha_L)(2-\alpha_L)\Delta+\beta_L(3-2\alpha_L)]}(\psi_L^e)''', \tag{34}$$

$$\tau_{\eta-1} = \frac{\Delta}{3}\alpha_R(\psi_{\eta-1}^e)''' + \frac{\beta_R(1-\alpha_R)(2-\alpha_R)\Delta}{3[(1-\alpha_R)(2-\alpha_R)\Delta+\beta_R(3-2\alpha_R)]}(\psi_R^e)'''. \tag{35}$$

In the Dirichlet case ($\beta_L=\beta_R=0$), Eqs. (30) and (31) reduce to those of [14], but note that there are two typographical errors in Eqs. (32) and (33) of [14]: in Eq. (32) the first summation should start from $j=2$ and in Eq. (33) $H_{N-1/2}$ should be the negative of the value given there.

For the linear boundary treatment by contrast

$$\xi_i = \Delta\left[\left(\frac{\beta_L+(i-\alpha_L)\Delta}{(\eta-\alpha_L-\alpha_R)\Delta+\beta_L+\beta_R}-1\right)\sum_{j=1}^{\eta-1}(\beta_L+(j-\alpha_L)\Delta)\tau_j-\Delta\sum_{j=i+1}^{\eta-1}(i-j)\tau_j\right]\quad\text{for } 1\leqslant i\leqslant\eta-1. \tag{36}$$

Again the error expression can be rewritten to isolate the terms similar to those found in the Dirichlet case from those approximately proportional to β as

$$\xi_i = \Delta^2\left[\left(\frac{(i-\alpha_L)\Delta}{(\eta-\alpha_L-\alpha_R)\Delta+\beta_L+\beta_R}-1\right)\sum_{j=1}^{\eta-1}(j-\alpha_L)\tau_j-\sum_{j=i+1}^{\eta-1}(i-j)\tau_j\right]$$
$$+(\beta_L\Delta)\left(\frac{\beta_L}{(\eta-\alpha_L-\alpha_R)\Delta+\beta_L+\beta_R}-1\right)\sum_{j=1}^{\eta-1}\tau_j\quad\text{for } 1\leqslant i\leqslant\eta-1, \tag{37}$$

where

$$\tau_1 = \frac{\alpha_L}{2}(\psi_1^e)'' - \frac{\beta_L(1-\alpha_L)}{2(\beta_L+(1-\alpha_L)\Delta)}(\psi_L^e)'',$$
$$\tau_{\eta-1} = \frac{\alpha_R}{2}(\psi_{\eta-1}^e)'' - \frac{\beta_R(1-\alpha_R)}{2(\beta_R+(1-\alpha_R)\Delta x)}(\psi_R^e)''. \tag{38}$$

Explicit forms for the 1D error for both quadratic and linear treatment of the boundary conditions are summarised in Table 1 for the special case $\beta=\beta_L=\beta_R$. When $\beta=0$ we recover the Dirichlet problem. As is well known, in this case both the quadratic and linear treatments give $\mathcal{O}(\Delta^2)$ error, but in general the coefficient of error is significantly larger for the linear case [14], so favouring the quadratic approach. For the more general Robin boundary conditions treated here, where $\beta\gg\Delta$,

Table 1
The order of the error for the two 1D cases: (a) quadratic treatment of boundary jumps and (b) linear treatment of boundary jumps.

(a) Quadratic	(b) Linear
$\tau_1 = \mathcal{O}(\Delta),\ \tau_{\eta-1} = \mathcal{O}(\Delta)$	$\tau_1 = \mathcal{O}(1),\ \tau_{\eta-1} = \mathcal{O}(1)$
$\tau_i = \mathcal{O}(\Delta^2),\ i = 2,\ldots,\eta-2$	$\tau_i = \mathcal{O}(\Delta^2),\ i = 2,\ldots,\eta-2$
$L\xi = \tau$	$L\xi = \tau$
$\mp\beta\frac{d\xi}{dx} + \xi = 0$ at $x = x_L$ and $x = x_R$	$\mp\beta\frac{d\xi}{dx} + \xi = 0$ at $x = x_L$ and $x = x_R$
$\xi_1 = \mathcal{O}(\Delta^2)\tau_1 + \mathcal{O}(\beta\Delta)\tau_1$	$\xi_1 = \mathcal{O}(\Delta^2)\tau_1 + \mathcal{O}(\beta\Delta)\tau_1$
$= \mathcal{O}(\Delta^3) + \mathcal{O}(\beta\Delta^2)$	$= \mathcal{O}(\Delta^2) + \mathcal{O}(\beta\Delta)$
$\xi_{\eta-1} = \mathcal{O}(\Delta^3) + \mathcal{O}(\beta\Delta^2)$	$\xi_{\eta-1} = \mathcal{O}(\Delta^2) + \mathcal{O}(\beta\Delta)$
$\xi_i = \mathcal{O}(\Delta^2)\sum i\tau_i + \mathcal{O}(\beta\Delta)\sum\tau_i$	$\xi_i = \mathcal{O}(\Delta^2)\sum i\tau_i + \mathcal{O}(\beta\Delta)\sum\tau_i$
$= \mathcal{O}(\Delta^2) + \mathcal{O}(\beta\Delta^2)$	$= \mathcal{O}(\Delta^2) + \mathcal{O}(\beta\Delta)$
$i = 2,\ldots,\eta-2$	$i = 2,\ldots,\eta-2$

the issue is more clearcut, because the linear approximation is now uniformly $\mathcal{O}(\beta\Delta)$ as opposed to the $\mathcal{O}(\beta\Delta^2)$ behaviour for the quadratic case. For the Dirichlet case, the 1D method can be applied dimension by dimension to build up the 2D and 3D methods, and so the 1D error expressions can be applied to give quantitative estimates of the error in these cases (see [14] for some 2D examples). For the Robin problem, the higher dimensional methods cannot be built in this way and so the 1D error estimates are only indicative of the behaviour to be expected. Despite this, the predictions of Table 1 are confirmed in the 2D and 3D numerical examples given in the next section.

For the 1D Dirichlet problem, the boundary error is $\mathcal{O}(\Delta^2), \mathcal{O}(\Delta^3)$ and $\mathcal{O}(\Delta^4)$ respectively for the linear boundary treatment, the quadratic boundary treatment and the special case of no boundary jumps i.e. where the boundary coincides or is aligned with a grid point (see Table 1 of [14]). However, in the Robin case the boundary error dominates the calculation due to the estimation of the derivative at the boundary points and gives $\mathcal{O}(\beta\Delta^2)$ and $\mathcal{O}(\beta\Delta)$ errors for the quadratic and the linear boundary treatments, respectively. For the aligned case, quadratic or linear discretisation of the Robin boundary condition can be used and results in $\mathcal{O}(\beta\Delta^2)$ or $\mathcal{O}(\beta\Delta)$ error, respectively. Estimating the derivative at a boundary point involves error which grows as the boundary point moves further from the point of discretisation, so that, for a given discretisation step, the aligned case has a larger coefficient of error than a non-aligned case. Consistent with our results, a 1D error analysis for the Dirichlet case gives $\mathcal{O}(\Delta^2)$ error in the immersed interface method [13] and the explicit-jump immersed interface method [27]. For more general boundary conditions, Ramière [24] finds $\mathcal{O}(\Delta^{1/2})$ error in the H^1-norm and this is shown to correspond to $\mathcal{O}(\Delta)$ in the L^2-norm for the Dirichlet case, but for this norm more general conditions were not treated. As stated in [24] the loss of one order of convergence in the L^2-norm is due to the use of a non-conforming mesh (staircase mesh).

3. Numerical results

In this section, we present results for two 3D problems in the unit sphere using the quadratic or linear boundary treatment described above. In each case, we solved the corresponding matrix problem using the conjugate gradient squared iteration method for sparse matrices as implemented in MATLAB: **cgs.m**. This was slightly faster for the problems treated here than the bi-conjugate gradient method (**bicg.m**) and the generalised minimum residual method (**gmres.m**), but no difficulties were encountered with any of these approaches. We then go to show two 2D problems in irregular domains and contrast the effects of using either the quadratic or linear boundary treatment.

3.1. 3D cases

In Fig. 2 we consider the problem of solving the Poisson equation $\nabla^2\psi = -3\cos(x+y+z)$ on the unit sphere, with Robin boundary conditions $\beta\frac{\partial\psi}{\partial n} + \psi = \gamma$, where γ is chosen so as to match exactly the left-hand side of the boundary condition. Outside the unit sphere we set $\psi = 0$. The domain is embedded in a cube of side length 2.5. The three columns are cross-sectional plots of the absolute error at $z = -1.25 + (j\eta/4)\Delta = -1.25 + 0.625j, j = 1\ldots3$, respectively, with $\eta = 80$, where η is the number of grid intervals in each coordinate direction.

First we show results for the Dirichlet case: row 1 (panels (a), (b) and (c)) corresponds to the quadratic case with $\beta = 0$ while in row 2 (panels (d), (e) and (f)) we show the corresponding linear treatment for $\beta = 0$. As reported in [14] the linear treatment, with apparent uniform $\mathcal{O}(\Delta^2)$ error, actually results in significant boundary errors. Similarly rows 3 and 4 give the quadratic and linear behaviour, respectively, for $\beta = 1$. As expected the error is much reduced with the quadratic treatment as opposed to the linear case and there is no particular tendency for boundary error to dominate, indicating consistency with the quadratic interior grid point treatment.

For the same problem, Fig. 3 shows the rms and maximum absolute errors as a function of η for $\eta = 10, 20, 40$ and 80. Panels (a), (b), (c) and (d) correspond to $\beta = 0, 0.1, 1$ and 10, respectively. The $\mathcal{O}(\beta\Delta^2)$ behaviour for the quadratic boundary treatment is very clear, with the error decreasing with the square of the number of grid intervals η in each direction and

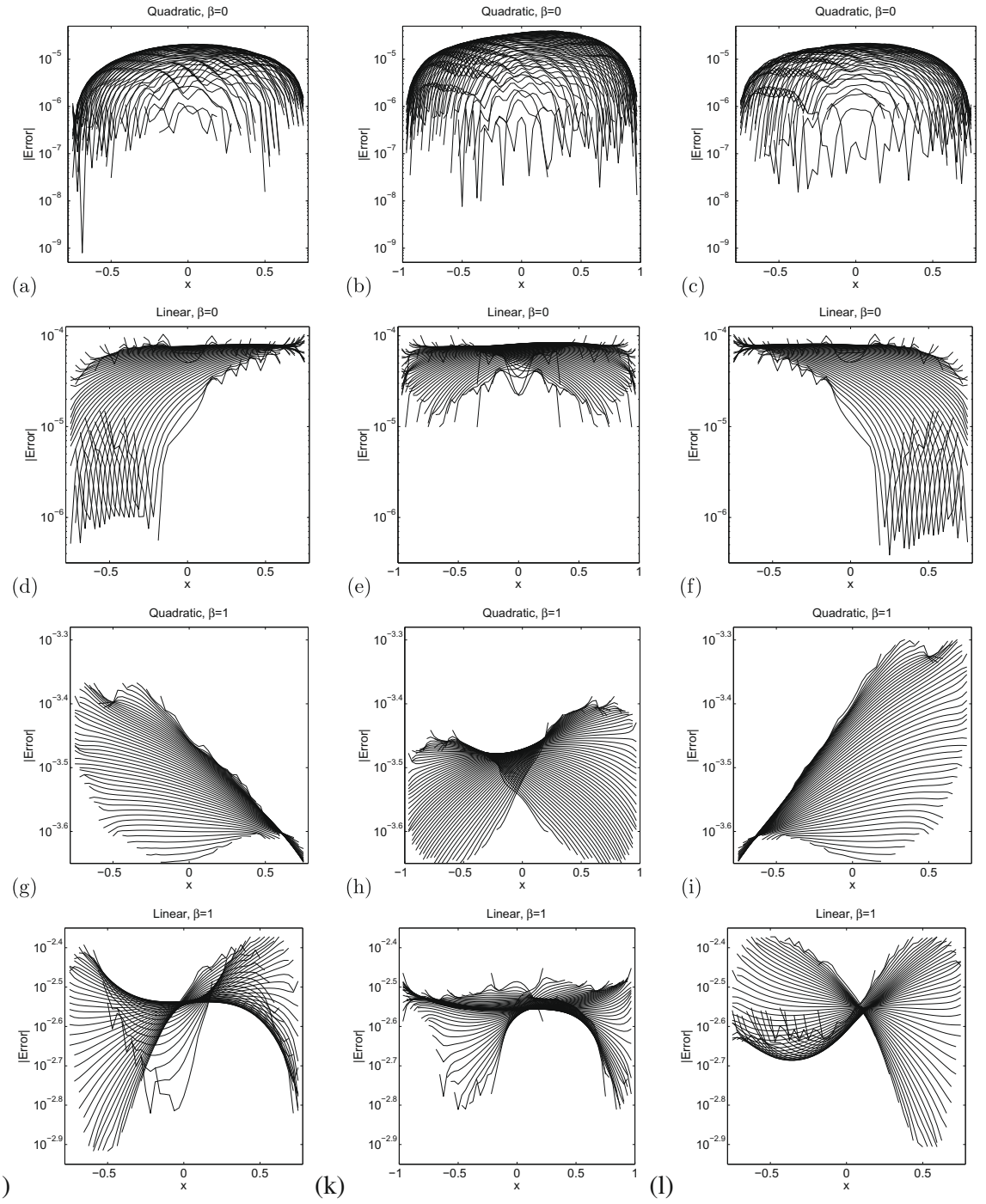

Fig. 2. The 3D problem $\nabla^2\psi = -3\cos(x+y+z)$, on the interior of the unit sphere, with $\beta\frac{\partial\psi}{\partial n} + \psi = \gamma$ on the boundary of the sphere and $\psi = 0$ elsewhere. Here $\eta\Delta = 2.5, \eta = 80$ and γ is chosen to match the left-hand side of the boundary condition. Columns one to three show cross-sectional plots of the absolute error at $z = -1.25 + j\frac{\eta}{4}\Delta, j = 1,\ldots,3 = -0.625, 0$ and 0.6255, respectively. The quadratic boundary treatment is shown in panels (a), (b) and (c) for $\beta = 0$ and in (g), (h) and (i) for $\beta = 1$. Similarly, the linear boundary treatment for $\beta = 0$ is shown in panels (d), (e) and (f) and for $\beta = 1$ in (j), (k) and (l).

linearly increasing through panels (b), (c) and (d) as β is increased, in agreement with the 1D analysis in Section 2.2, Eq. (30). We see that the coefficient of error for the Robin case is always significantly greater than for the corresponding Dirichlet problem. The linear treatment shows $\mathcal{O}(\beta\Delta)$ behaviour as in Eq. (36).

In Table 2, we compare the maximum absolute error and the CPU time for both quadratic and linear treatments in the special case $\beta = 1$ using the MATLAB routine **cgs.m** (including matrix setup time and with no preconditioner). The results

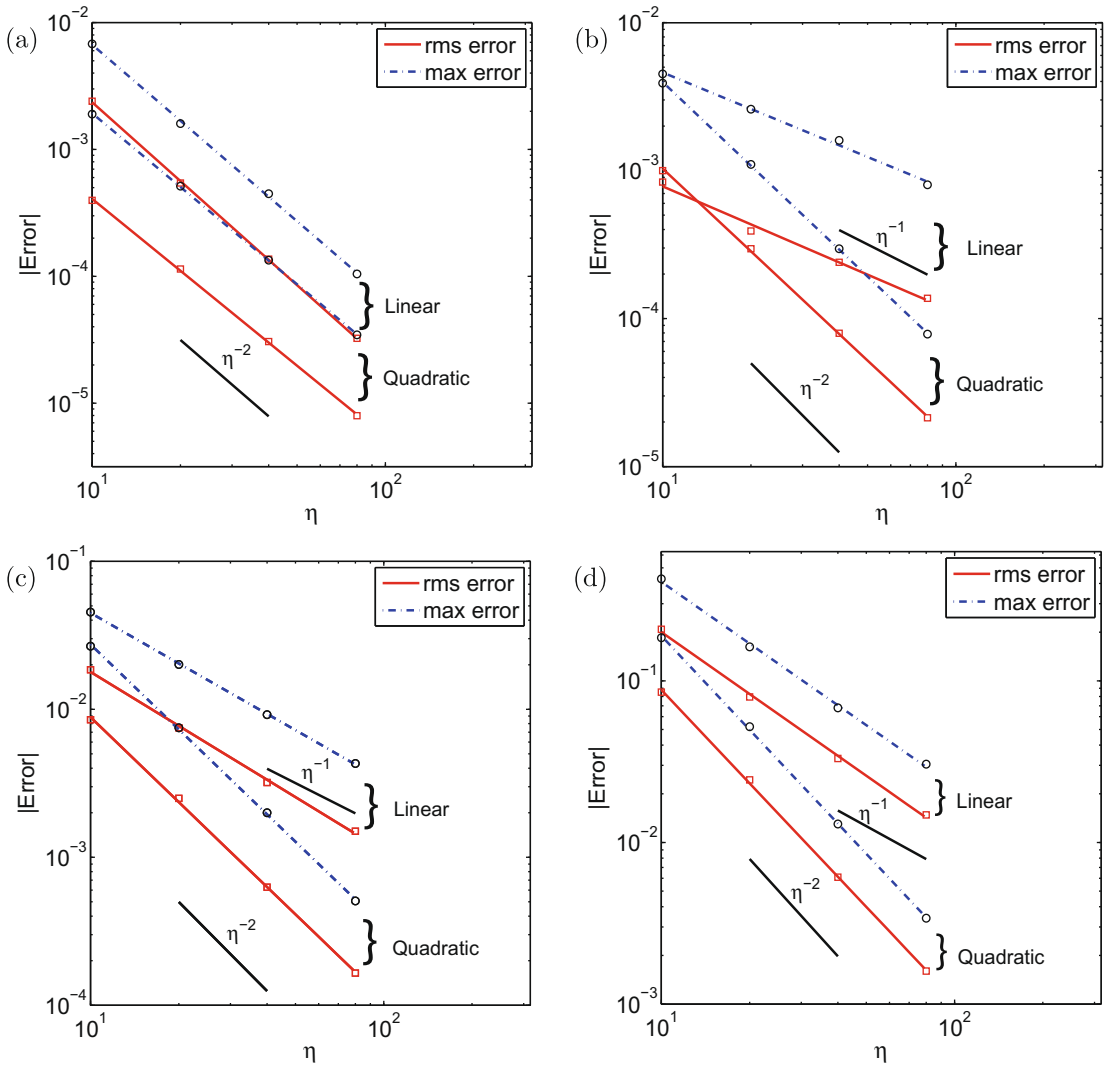

Fig. 3. For the problem treated in Fig. 2, for the quadratic and linear boundary treatment, panels (a)–(d) show the rms errors (solid lines) and maximum absolute errors (dash-dotted lines) as a function of η, where $\eta\Delta = 2.5$ and $\beta = 0, 0.1, 1$ and 10, respectively.

Table 2
The maximum absolute error and the CPU time for the 3D cases $\nabla^2\psi = -3\cos(x+y+z)$ on the unit sphere subject to Robin boundary conditions and $\beta = 1$: (a) quadratic, (b) linear.

η	(a) Quadratic		(b) Linear	
	Max |error|	CPU time	Max |error|	CPU time
10	0.0267	0.033	0.0454	0.0299
20	0.0075	0.29	0.0201	0.205
40	0.002	7.3	0.0092	4.7
80	5.1e−4	471	0.0043	230

show that for the same number of grid intervals the CPU time needed for the quadratic boundary treatment is approximately twice as much as that needed for the linear boundary treatment. However, this is not significant once the increased accuracy of the quadratic method is taken into account. We also used the standard **A****b** MATLAB command for $\eta = 40$, which automatically invokes the **umfpack** routines for large sparse matrices: however, we found that this was slower. In fact the routine failed for larger values of η, partly due to insufficient memory problems.

Figs. 4 and 5 are similar to Figs. 2 and 3, respectively, but for the 3D problem $\nabla^2\psi = \exp(x+z)\cos y$. The presence of the exponential function on the right-hand side of the Poisson equation does not appear to affect conclusions about the convergence. Indeed, numerical experiments with a broad range of functions give similar results.

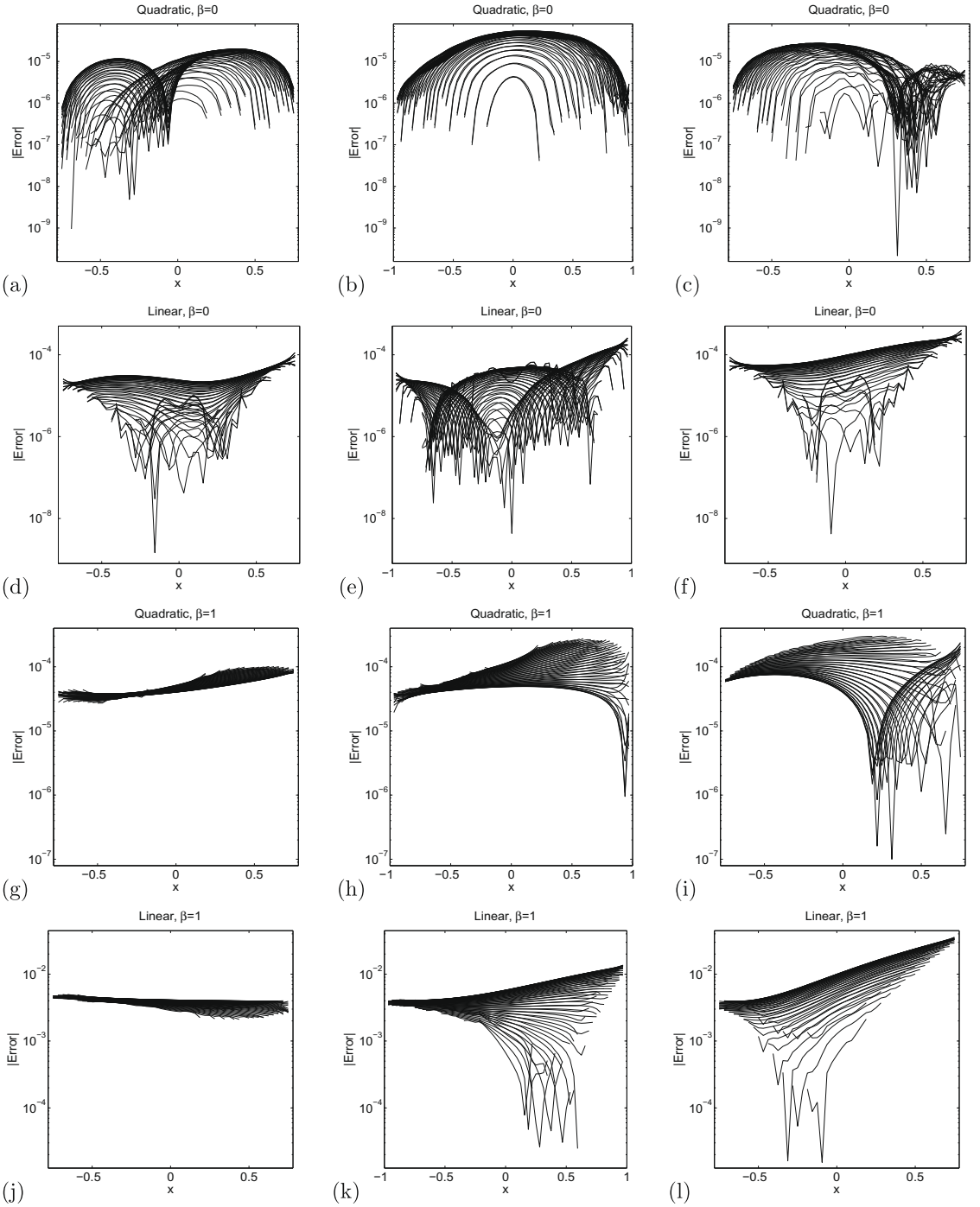

Fig. 4. The 3D problem $\nabla^2\psi = \exp(x+z)\cos y$ in the interior of the unit sphere, subject to $\beta\frac{\partial\psi}{\partial n} + \psi = \gamma$ on the boundary of the sphere and $\psi = 0$ elsewhere. Here $\eta\Delta = 2.5$, $\eta = 80$ and γ is chosen to match the left-hand side of the boundary condition. Columns one to three show cross-sectional plots of the absolute error at $z = -1.25 + j\frac{\eta}{4}\Delta, j = 1,\ldots,3 = -0.625, 0$ and 0.625, respectively. The quadratic boundary treatment is shown in panels (a), (b) and (c) for $\beta = 0$ and in (g), (h) and (i) for $\beta = 1$. Similarly, the linear boundary treatment for $\beta = 0$ is shown in panels (d), (e) and (f) and for $\beta = 1$ in (j), (k) and (l).

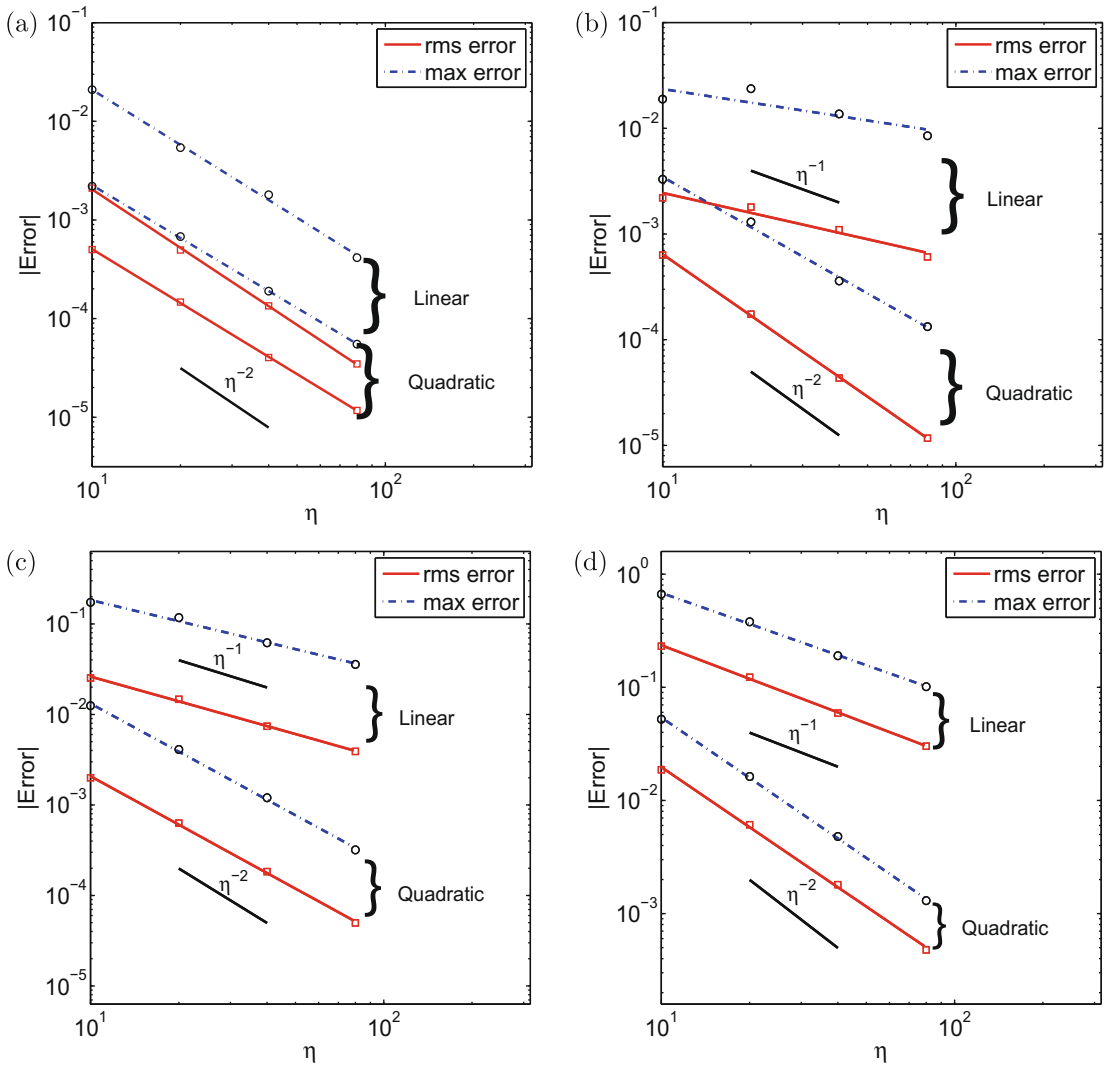

Fig. 5. For the problem treated in Fig. 4, for the quadratic and linear boundary treatment, panels (a)–(d) show the rms errors (solid lines) and maximum absolute errors (dash-dotted lines) as a function of η, where $\eta\Delta = 2.5$ for $\beta = 0, 0.1, 1$ and 10, respectively.

3.2. 2D cases

In Fig. 6 we consider the problem of inverting the Poisson equation $\nabla^2\psi = 7r^2\cos 3\theta$, subject to $\beta\frac{\partial\psi}{\partial n} + \psi = \gamma$ on the boundary of the six-leafed shape described by $r = 0.3 + 0.15\cos 6\theta$. We set $\psi = 0$ outside this domain. Here γ is chosen to match the left-hand side of the boundary conditions. The domain is embedded in a square of side length one, with $\eta\Delta = 1$ and $\eta = 100$. Panels (a) and (b) show plots of the absolute errors for the quadratic and linear treatments with a Dirichlet boundary condition ($\beta = 0$) whereas panels (d) and (e) deal with the corresponding Robin case where $\beta = 1$. We plot the rms and maximum errors for $\beta = 0, 0.1, 1$ and 10 in panels (c), (f), (h) and (i), for $\eta = 40, 80, 160$ and 320 for both the quadratic and linear boundary treatments. Panel (g) shows the region. Again we see that the quadratic boundary method for the Robin condition (panel (e)) is better than the linear method but that the errors for the Dirichlet case are significantly smaller. The behaviour is qualitatively similar to the 3D test cases, with the quadratic error scaling like $\mathcal{O}(\beta\Delta^2)$, and the linear error clearly scaling like $\mathcal{O}(\beta\Delta)$, as suggested by the 1D analysis.

The second 2D example in Fig. 7 is for the case $\nabla^2\psi = e^x(y^2 + 2(1 + 2x)\sin y + 2)$, $\eta\Delta = 1.7096$ and $\eta = 100$ with the irregular domain described by $x = 0.613\cos\theta - 0.27\cos 3\theta, y = 0.712\sin\theta - 0.06\sin 3\theta + 0.05\sin 7\theta$, where $\beta = 0$ for the dashed-line and $\beta = 1$ for the solid line (see panel (g)). The panels correspond to those in Fig. 6 and the behaviour is qualitatively similar. Panels corresponding to the rms and maximum errors are similar to those in Fig. 6, but the value of β is zero for the dashed part of the boundary and 0, 0.1, 1 and 10, respectively, for the solid part of the boundary. The rms and maximum errors again show very similar qualitative behaviour.

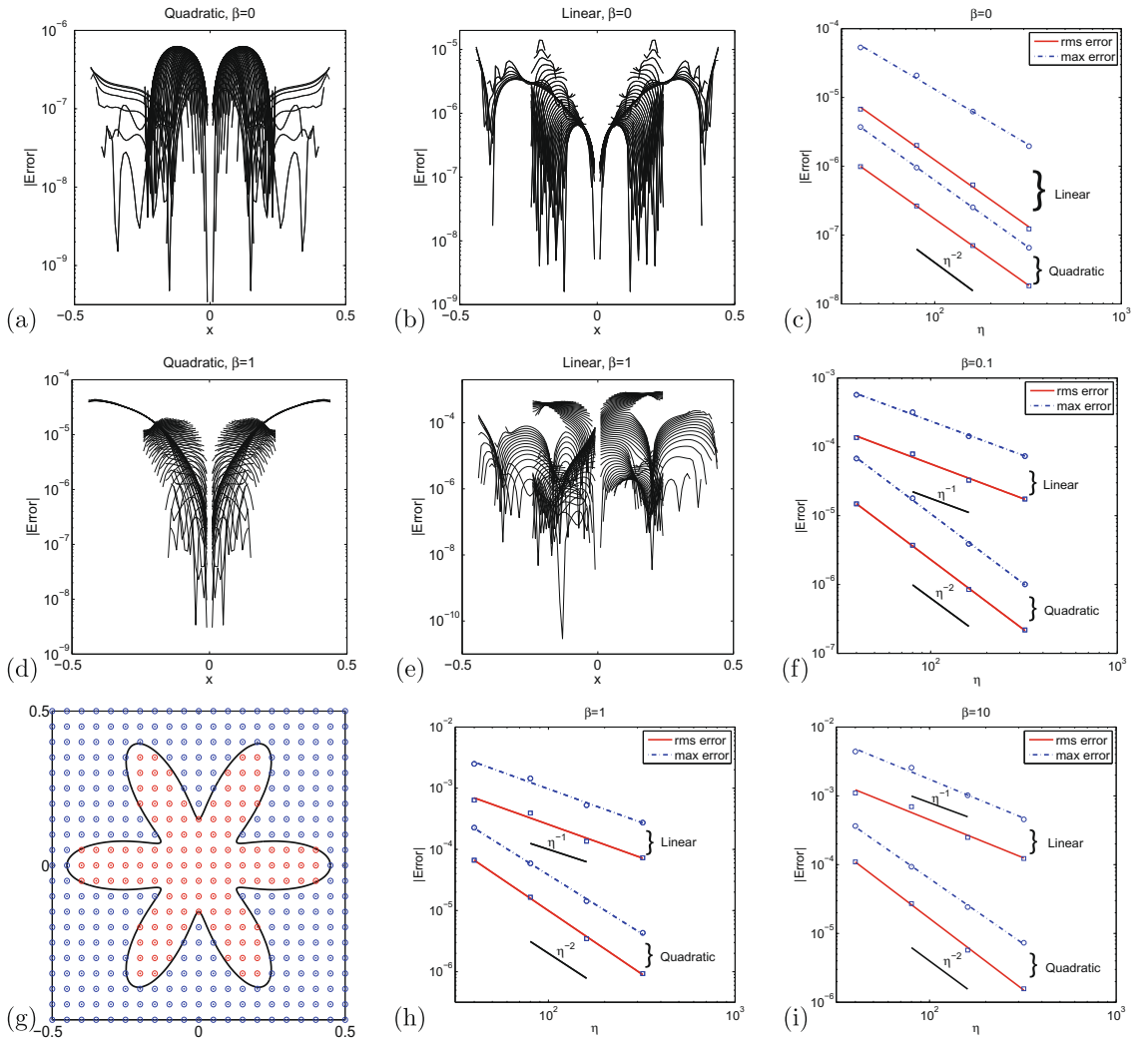

Fig. 6. The 2D problem $\nabla^2\psi = 7r^2\cos 3\theta$ in the interior of the six-leafed shape (see panel (g)) described by $r = 0.3 + 0.15\cos 6\theta$, subject to $\beta\frac{\partial\psi}{\partial n} + \psi = \gamma$ on the boundary and with $\psi = 0$ elsewhere. Here γ is chosen to match the left-hand side of the boundary condition, $\eta\Delta = 1$ and $\eta = 100$. The numerical error for the quadratic boundary treatment is shown for (a) $\beta = 0$ and (d) $\beta = 1$ and for the linear boundary treatment in (b) $\beta = 0$ and (e) $\beta = 1$. Panels (c), (f), (h) and (i) compare the rms errors (solid lines) and maximum absolute errors (dash-dotted lines) for the quadratic and linear boundary treatments with $\beta = 0, 0.1, 1$ and 10, respectively.

4. Conclusion

In this paper we have presented a second-order accurate method for the solution of the Poisson equation, subject to Robin boundary conditions, on an irregular 3D domain embedded in a regular 3D mesh of grid points. The method extends the well-known Shortley–Weller approach for the Dirichlet problem [25]. However, this extension needs to be addressed for 1D, 2D and 3D separately, since the Robin formulation is not additive, by contrast with the Dirichlet case. In addition, the quadratic boundary treatment requires a quadratic discretisation of the normal derivative appearing in the Robin boundary condition in order to maintain the $O(\Delta^2)$ accuracy. The technique is derived using a Taylor series approach, but is shown to agree with a simpler geometric derivation in the 2D case [15]. In the 2D case, the results can be shown to be consistent with those in [12], derived by similar methods but for a variation on the boundary conditions treated here. In the 1D case, where the boundary conditions are $\mp\beta d\psi/dx + \psi = \gamma$ for the left-hand and right-hand boundaries respectively, the error involved with this quadratic treatment is uniformly $\mathcal{O}(\Delta^2) + \mathcal{O}(\beta\Delta^2)$ whereas a linear treatment of the boundary conditions gives error of $\mathcal{O}(\Delta^2) + \mathcal{O}(\beta\Delta)$. Although this analysis is not directly relevant to the 2D and 3D cases, numerical experiments indicate similar scaling of error for a range of test cases. Unlike some methods previously derived for the 2D problem [4,21,3], the current technique does not give rise to a coefficient matrix that is an M-matrix. This is a significant deficiency for iterative solution. However, the technique described here only involves nodes on the cube of side 2Δ centred on the node of interest.

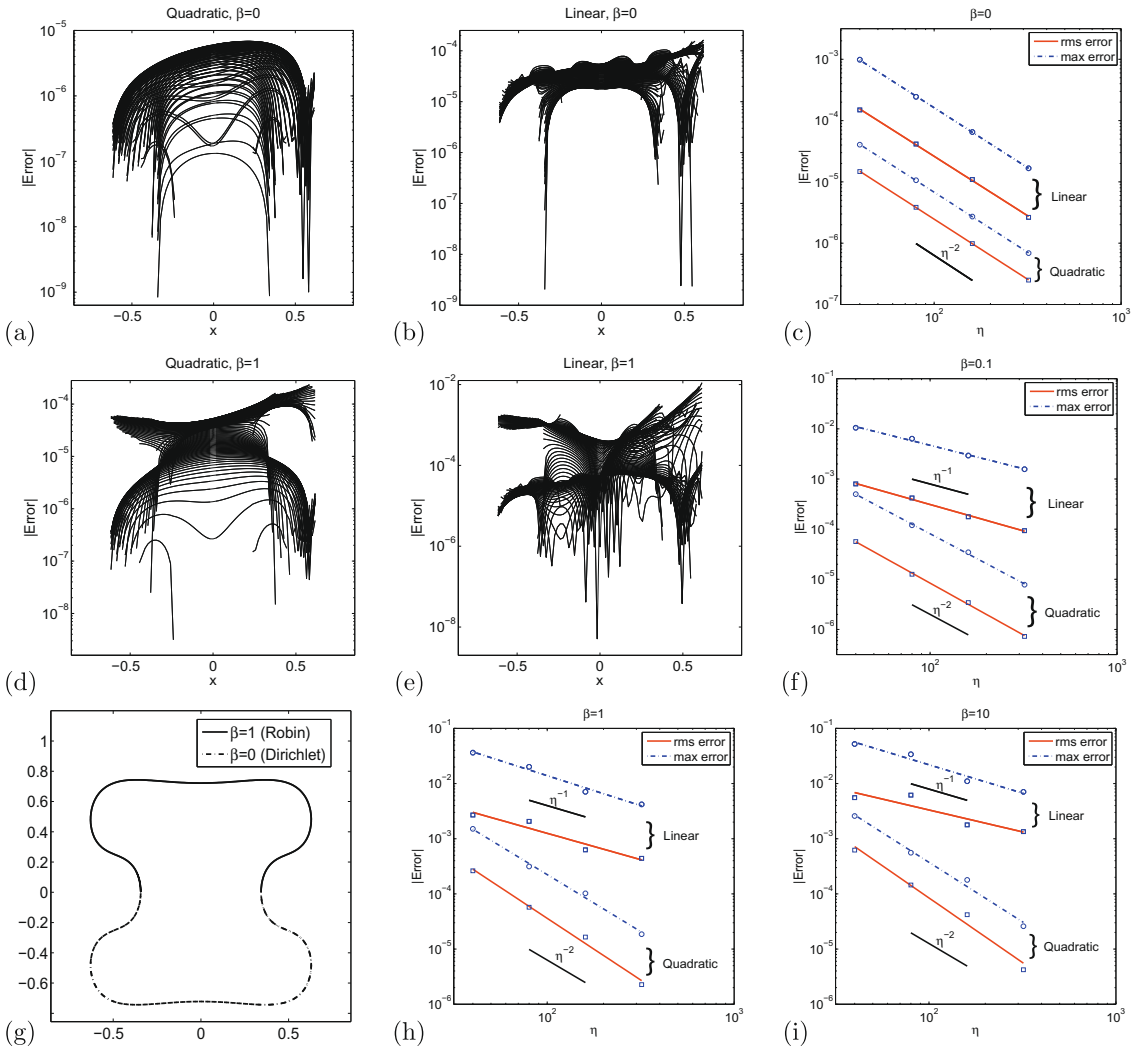

Fig. 7. The 2D problem $\nabla^2\psi = (y^2 + 2(1+2x)\sin y + 2)\exp(x)$ on the interior of the shape described by $x = 0.613\cos\theta - 0.27\cos 3\theta, y = 0.712\sin\theta - 0.06\sin 3\theta + 0.05\sin 7\theta$ (see panel (g)), subject to $\beta\frac{\partial\psi}{\partial n} + \psi = \gamma$ on the boundary ($\beta = 0$ for the dashed line and $\beta = 1$ for the solid line) and with $\psi = 0$ elsewhere. γ is chosen to match the left-hand side of the boundary condition, $\eta\Delta = 1.7096$ and $\eta = 100$. The numerical error for the quadratic boundary treatment is shown for (a) $\beta = 0$ and (d) $\beta = 1$ for the portion of the boundary shown as a solid line. The corresponding linear boundary treatment results are shown for (b) $\beta = 0$ and (e) $\beta = 1$. Panels (c), (f), (h) and (i) compare the rms errors (solid lines) and maximum absolute errors (dash-dotted lines) for the quadratic and linear boundary treatments with $\beta = 0, 0.1, 1$ and 10, respectively, on the part of the boundary drawn with a solid line.

Acknowledgements

We thank Professor David Dritschel, who suggested the approach taken in this paper.

Appendix A. The *N*-dimensional case

The N-dimensional problem $(N > 2)$ leads to the following system of equations:

$$\begin{pmatrix} I & BG & \Delta B(I-A)F_{N,M} & 2\Delta B(I-A)D \\ 0 & \Delta I & 0 & -\Delta^2 I \\ 0 & \Delta K_{M,N} & -\Delta^2 I_M & -\Delta^2 K_{M,N} \\ I & -\Delta(I-A) & 0 & -\Delta^2(I-A)^2 \end{pmatrix} \begin{pmatrix} \psi \\ c \end{pmatrix} = \begin{pmatrix} \gamma \\ p_1 \\ p_2 \\ p_3 \end{pmatrix}, \tag{A.1}$$

where $M = N(N-1)/2$. In (A.1) ψ is a vector of N elements, c is the vector of $N(N+3)/2$ constants in the Taylor expansion of ψ, γ is a vector of N elements, I is the $N \times N$ identity matrix, and A, B and D are $N \times N$ diagonal matrices where

$$A_{rq} = \alpha_r \delta_{rq}, \quad B_{rq} = \beta_r \delta_{rq} \quad \text{and} \quad D_{rq} = n_{rr} \delta_{rq}. \tag{A.2}$$

I_M is the identity matrix of order M and G is an $N \times N$ matrix with $G_{rq} = n_{rq}$, where n_{rq} is the component of the normal at the rth jump in the qth direction.

$F_{N,M}$ is an $N \times M$ matrix, defined recursively by

$$F_{N,M} = \begin{pmatrix} & & \begin{pmatrix} n_{1N} & 0 & 0 & \dots & 0 \\ 0 & n_{2N} & 0 & \dots & 0 \\ \vdots & 0 & \ddots & 0 & \vdots \\ 0 & \vdots & \vdots & \ddots & 0 \\ 0 & 0 & 0 & \dots & n_{N-1N} \end{pmatrix} \\ F_{N-1,M} & & \\ & & \\ (0 \quad \dots \quad 0) & & (n_{N1} \quad n_{N2} \quad \dots \quad \dots \quad n_{NN-1}) \end{pmatrix}. \tag{A.3}$$

$K_{M,N}$ is an $M \times N$ matrix, with transpose $K_{N,M}$ defined recursively by

$$K_{N,M} = \begin{pmatrix} K_{N-1,M} & & I_{N-1} & & \\ (0 \quad \dots \quad 0) & (1 & 1 \quad \dots \quad \dots & 1) \end{pmatrix}. \tag{A.4}$$

Here p_1 and p_3 are vectors of length N, while p_2 is a vector of length M:

$$p_1 = \begin{pmatrix} \psi_{i_1,i_2,\dots,i_N} - \psi_{i_1-1,i_2,\dots,i_N} \\ \psi_{i_1,i_2,\dots,i_N} - \psi_{i_1,i_2-1,\dots,i_N} \\ \vdots \\ \psi_{i_1,i_2,\dots,i_N} - \psi_{i_1,i_2,\dots,i_N-1} \end{pmatrix}, \quad p_2 = \begin{pmatrix} \psi_{i_1,i_2,\dots,i_N} - \psi_{i_1-1,i_2-1,i_3,\dots,i_N} \\ \psi_{i_1,i_2,\dots,i_N} - \psi_{i_1-1,i_2,i_3-1,\dots,i_N} \\ \vdots \\ \psi_{i_1,i_2,\dots,i_N} - \psi_{i_1,i_2,\dots,i_{N-1}-1,i_N-1} \end{pmatrix},$$

$$p_3 = \psi_{i_1,i_2,\dots,i_N} \begin{pmatrix} 1 \\ \vdots \\ 1 \end{pmatrix}. \tag{A.5}$$

Here $i_1, i_2, \dots, i_N$ are the indices of the N dimensions, generalising the (i,j,k) notation used in the body of the paper. By row operations following those given for the $N = 3$ case in the body of the paper (A.1) can be reduced to the system of equations

$$\begin{pmatrix} I+E & 0 & 0 & 0 \\ I & -\Delta(I-A)(2I-A) & 0 & 0 \\ 0 & 0 & \Delta^2 I_M & 0 \\ I & -\Delta(I-A) & 0 & -\Delta^2(I-A)^2 \end{pmatrix} \begin{pmatrix} \psi \\ c \end{pmatrix} = \begin{pmatrix} p_6 \\ p_5 \\ p_4 \\ p_3 \end{pmatrix}, \tag{A.6}$$

where

$$E_{rq} = \frac{\beta_r (1 + 2\delta_{rq}(1-\alpha_q)) n_{rq}}{\Delta(1-\alpha_q)(2-\alpha_q)}, \quad r, q = 1, 2, \dots, N, \tag{A.7}$$

and

$$p_4 = \begin{pmatrix} \psi_{i_1-1,i_2-1,i_3,\dots,i_N} + \psi_{i_1,i_2,i_3,\dots,i_N} - \psi_{i_1-1,i_2,i_3,\dots,i_N} - \psi_{i_1,i_2-1,i_3,\dots,i_N} \\ \psi_{i_1-1,i_2,i_3-1,\dots,i_N} + \psi_{i_1,i_2,i_3,\dots,i_N} - \psi_{i_1-1,i_2,i_3,\dots,i_N} - \psi_{i_1,i_2,i_3-1,\dots,i_N} \\ \vdots \\ \psi_{i_1,i_2,i_3,\dots,i_{N-1}-1,i_N-1} + \psi_{i_1,i_2,i_3,\dots,i_{N-1},i_N} - \psi_{i_1,i_2,\dots,i_{N-1}-1,i_N} - \psi_{i_1,i_2,\dots,i_{N-1},i_N-1} \end{pmatrix},$$

$$p_5 = (I-A)^2 \begin{pmatrix} \psi_{i_1-1,i_2,i_3,\dots,i_N} \\ \psi_{i_1,i_2-1,i_3,\dots,i_N} \\ \vdots \\ \psi_{i_1,i_2,\dots,i_{N-1},i_N-1} \end{pmatrix} + A(2I-A)p_3,$$

$$p_6 = \gamma + \frac{1}{\Delta} B(I-A)(2Dp_1 - F_{N,M}p_4) + Ep_5. \tag{A.8}$$

References

[1] K. Balakrishnan, P.A. Ramachandran, Osculatory interpolation in the method of fundamental solution for nonlinear Poisson problems, J. Comput. Phys. 172 (2001) 1–18.

[2] V.E. Batschelet, Über die numerische Auflosung von randwert problem bei elliptischen partiellen differentialgleichungen, Z. Angew. Math. Phys. 3 (1952) 165–193.
[3] F. Bouchon, G.H. Peichl, A second-order immersed interface technique for an elliptic Neumann problem, Numer. Methods Partial Differ. Equat. 23 (2007) 400–420.
[4] J.H. Bramble, B.E. Hubbard, Approximation of solutions of mixed boundary value problems for Poisson's equation by finite differences, J. Assoc. Comput. Mach. 12/1 (1965) 114–123.
[5] J.H. Bramble, B.E. Hubbard, A finite difference analogue of the Neumann problem for Poisson's equation, J. Soc. Indust. Appl. Math. Ser. B Numer. Anal. 2 (1965) 1–14.
[6] P.G. Ciarlet, Introduction to Numerical Linear Algebra and Optimization, 1st English ed., Cambridge University Press, 1989.
[7] L. Collatz, Bemerkungen zur fehlerabschätzung für das differnzenverfahren bei partiellen differentialgleichungen, Z. Angew. Math. Mech. 13 (1933) 56–57.
[8] M.A. Dumett, J.P. Keener, An immersed interface method for anisotropic elliptic problems on irregular domains in 2D, Numer. Methods Partial Differ. Equat. 21 (2) (2005) 397–420.
[9] M.A. Dumett, J.P. Keener, An immersed interface method for solving anisotropic elliptic boundary value problems in three dimensions, SIAM J. Sci. Comput. 25 (1) (2003) 348–367.
[10] Q. Fang, T. Yamamoto, Superconvergence of finite difference approximations for convection–diffusion problems, Numer. Linear Algebra Appl. 8 (2001) 99–110.
[11] L. Fox, Numerical Solution of Ordinary and Partial Differential Equations, Pergamon Press, Oxford, 1962.
[12] D. Greenspan, On the numerical solution of problems allowing mixed boundary conditions, J. Franklin Inst. 277 (1964) 11–30.
[13] H. Huang, Z. Li, Convergence analysis of the immersed interface method, IMA J. Numer. Anal. 19 (1999) 583–608.
[14] Z. Jomaa, C. Macaskill, The embedded finite difference method for the Poisson equation in a domain with an irregular boundary and Dirichlet boundary conditions, J. Comput. Phys. 202 (2005) 488–506.
[15] Z. Jomaa, C. Macaskill, Numerical solution of the 2D Poisson equation on an irregular domain with Robin boundary conditions, Proc. CTAC 2008, ANZIAM J. 50 (2008) C413–C428.
[16] H. Johansen, P. Colella, A Cartesian grid embedded boundary method for Poisson's equation on irregular domains, J. Comput. Phys. 147 (1998) 60–85.
[17] R.J. LeVeque, Z. Li, The immersed interface method for elliptic equations with discontinuous coefficients and singular sources, SIAM J. Numer. Anal. 31 (1994) 1019–1044.
[18] H.J. Van Linde, High-order finite-difference methods for Poisson's equation, Math. Comput. 28 (1974) 369–391.
[19] X. Liu, R. Fedkiw, M. Kang, A boundary condition capturing method for Poisson's equation on irregular domains, J. Comput. Phys. 160 (2000) 151–178.
[20] N. Matsunaga, T. Yamamoto, Superconvergence of the Shortley–Weller approximation for Dirichlet problems, J. Comput. Appl. Math. 116 (2000) 263–273.
[21] G.H. Peichl, An immersed interface technique for mixed boundary value problems, in: Proceedings of the SEAMS-GMU Conference 2003, Yogyakarta, pp. 14–23.
[22] I. Ramière, P. Angot, M. Belliard, A general fictitious domain method with immersed jumps and multilevel nested structured meshes, J. Comput. Phys. 225 (2007) 1347–1387.
[23] I. Ramière, P. Angot, M. Belliard, A fictitious domain approach with spread interface for elliptic problems with general boundary conditions, Comput. Meth. Appl. Mech. Eng. 196 (2007) 766–781.
[24] I. Ramière, Convergence analysis of the Q_1-finite element method for elliptic problems with non-boundary-fitted meshes, Int. J. Numer. Meth. Eng. 75 (2008) 1007–1052.
[25] G.H. Shortley, R. Weller, The numerical solution of Laplace's equation, J. Appl. Phys. 9 (1938) 334–348.
[26] R.V. Viswanathan, Solution of Poisson's equation by relaxation method – normal gradient specified on curves boundaries, Math. Tables Aids Comput. 11 (1957) 67–78.
[27] A. Wiegmann, K.P. Bube, The explicit-jump immersed interface method: finite difference methods for PDEs with piecewise smooth solutions, SIAM J. Numer. Anal. 37 (2000) 827–862.